Dislocation-mediated creep process in nanocrystalline Cu*

Mu Jun-Wei(穆君伟), Sun Shi-Cheng(孙世成), Jiang Zhong-Hao(江忠浩)†,
Lian Jian-She(连建设), and Jiang Qing(蒋 青)

Key Laboratory of Automobile Materials, Department of Materials Science and Engineering, Jilin University, Changchun 130025, *China*

(Received 6 November 2012; revised manuscript received 17 December 2012)

Nanocrystalline Cu with average grain sizes ranging from ∼ 24.4 to 131.3 nm were prepared by the electric brush-plating technique. Nanoindentation tests were performed within a wide strain rate range, and the creep process of nanocrystalline Cu during the holding period and its relationship to dislocation and twin structures were examined. It was demonstrated that creep strain and creep strain rate are considerably significant for smaller grain sizes and higher loading strain rates, and are far higher than those predicted by the models of Cobble creep and grain boundary sliding. The analysis based on the calculations and experiments reveals that the significant creep deformation arises from the rapid absorption of high density dislocations stored in the loading regime. Our experiments imply that stored dislocations during loading are highly unstable and dislocation activity can proceed and lead to significant post-loading plasticity.

Keywords: nanocrystalline, creep, dislocation, nanoindentation

PACS: 73.63.Bd, 62.20.Hg, 61.72.Lk, 62.90.+k **DOI:** 10.1088/1674-1056/22/3/037303

1. Introduction

The plastic deformation of coarse grained (CG) metals is mediated by nucleation and movement of intragranular dislocations. Interactions of dislocations on intersecting slip planes create a permanent dislocation network that hinders further movement of dislocations, and thus hardens materials. However, as suggested by molecular dynamics (MD) simulations.[1–4] and experiments,[5–7] such dislocation activity is no longer possible in metals when the grain size is reduced to nanometer level and is replaced by the emission of dislocations from grain boundary (GB) sources. The emitted dislocations will propagate across the grains and eventually be absorbed in the opposite GBs. It is well known that as the grain size of crystals d decreases, the yield strength σ of the crystals increases.[8] This relationship is the empirical Hall–Petch relationship (abbreviated as the H-P relation):[9,10]

$$\sigma_y = \sigma_0 + kd^{-1/2}, \tag{1}$$

where σ_0 is the friction stress, and k is a material-dependent constant. Since $H_y \approx 3\sigma_y$,[11] it follows that equation (1) may be replaced by

$$H_y = H_0 + k_{\mathrm{H}} d^{-1/2}, \tag{2}$$

where H_0 and k_{H} are appropriate constants associated with the hardness measurements. This relationship is very well established for materials with large grain sizes and it serves to demonstrate that the hardness increases monotonically with decreasing the average grain size d for a fixed k value. As reported by Xu *et al.*,[12] CG Cu has small strain rate sensitivity. With the decrease of the grain size to the nanometer range, the yield strength σ or hardness H tends to be sensitive to strain rate.[13,14] However, the relationship between k value and strain rate has not been shown experimentally. At the same time, most studies on the H–P relation focus on the relationship between grain size and strength[14] or hardness.[14,15] The effect of grain size on the dislocation activity and deformation process of polycrystalline materials has not been fully studied yet, because it is difficult to prepare samples with different grain sizes using the same method and experimentally observe the dislocation activity in nanocrystalline (NC) materials. The high mobility and short lifetime of emitted dislocations from GBs make traditional transmission electron microscope (TEM) techniques unable to capture the dislocation structure in deformed nc metal because of its inevitable relaxation during film sample preparation. On the other hand, GB-mediated process such as GB sliding and GB diffusion can take place concurrently with the dislocation activity.[2,3,16] Complicated interactions between these mechanisms also result in difficulties in identifying which of them dominates in a mechanical experiment with a given experimental condition. In recent years, nanoindentation has been widely applied to study the deformation of NC materials and provide accurate consecutive measurements of the indentation load and penetration depth.[4,5,15,17] It should be noticed that the effective dislocation storage would occur only at sufficiently large indenter depth and a high enough loading strain rate.[5,18]

In this study, NC Cu samples with different grain sizes

*Project supported by the National Natural Science Foundation of China (Grant Nos. 50771049 and 50871046) and the National Basic Research Program of China (Grant No. 2010CB631001).

†Corresponding author. E-mail: jzh@jlu.edu.cn

© 2013 Chinese Physical Society and IOP Publishing Ltd

were prepared using the same method, i.e., the electric brush-plating technique. The creep behaviors were examined by performing nanoindentation tests loading at a large indenter depth and a broad loading strain rate range. A variety of k values with the strain rate were investigated at the nanometer grain sizes level. The deformation or dislocation structures in the NC Cu were connected with the creep behavior observed in the holding regime. A primary aim of this study is to examine the dislocation activity and relevant plastic deformation behavior after loading so as to obtain an overall understanding of the grain size and strain rate influence on the deformation process.

2. Experimental details

The bulk NC Cu used in this test was prepared using a bath mainly containing $CuSO_4$ (100–300 g/l), NH_4NO_3 (30 g/l), citric acid (3 g/l), and few additives. The brush-plating operation was carried out at room temperature on a brush-plating system developed recently.[5,19] In order to obtain NC Cu with different average grain sizes, different current densities, and concentration of $CuSO_4$ in the bath (1338.6 mA/cm^2, 300 g/l; 690.3 mA/cm^2, 300 g/l; 251.8 mA/cm^2, 300 g/l; 251.8 mA/cm^2, 200 g/l; 251.8 mA/cm^2, 100 g/l) were used. The purity and density of these NC Cu were $\sim$ 99.7 wt.% and $\sim$ 8.95 g/cm^3, respectively.

Nanoindentation tests were performed at room temperature on an Agilent Nanoindenter G200 with a Berkovich diamond indenter. The samples used for the nanoindentation tests have a thickness of $\sim$ 0.2 mm and an area of $\sim$ 8 mm$\times$8 mm with their test surfaces mechanically polished. The samples were indented at a loading strain rate from 10^{-3} s^{-1} to 4×10^{-1} s^{-1} to a depth of 2000 nm and were held at maximum load for 200 s, and then samples were unloaded to 10% of the maximum load by using the same unloading strain rate of 4×10^{-1} s^{-1}. Indentation was repeated at least ten times for each measurement.

The TEM microstructure of the NC Cu samples was examined on a JEM-2100F. film sampler before nanoindentation tests for the TEM examination were treated with a normal method. Film samples after nanoindentation tests were first mechanically grounded to a thickness of $\sim$ 20 μm and then cut to disks of 3 mm in diameter, which were polished on both sides to obtain a surface suitable for nanoindentation. Next, the samples were transferred to the nanoindenter and approximately 100 indents were placed in a geometrical array on the flat surface. Finally, the samples were thinned to a thickness of electron transparency. The 101 rapid etching system (RES) has two ion guns for thinning both surfaces of samples at the same time, but in this thinning process, the gun which is used for thinning the surface with indentations was shut down after working for 25 min in order to avoid thinning of indentations. Then, the other gun continued to work until the end. To affirm that the region is an indentation position, scanning electron microscope (SEM) of the NC Cu sample for TEM examination was examined on a JSM-5600.

3. Results

3.1. Nanoindentation results

Nanoindentation experiments were conducted on five NC Cu samples prepared using the brush-plating method with five different average grain sizes (d): $\sim$ 24.4 nm, $\sim$ 53.7 nm, $\sim$ 71.2 nm, $\sim$ 93.3 nm, and $\sim$ 131.3 nm. More details of the microstructure are provided below.

3.1.1. Strain rate sensitivity and H–P relation for the NC Cu

Figures 1(a)–1(e) show the representative load–displacement (P–h) curves for the five NC Cu with different grain sizes obtained for loading strain rates ($\dot{\varepsilon}_L$) from $10^{-3}$to 4×10^{-1} s^{-1}, indenter depth of 2000 nm, and holding time of 200 s. In the loading regime, the load required for a given indenter displacement increases more obviously at small grain size than that at large grain size with the increasing $\dot{\varepsilon}_L$. This indicates an increasing strain rate sensitivity of hardness or stress of these NC Cu with decreasing grain sizes, which can be evaluated by the strain rate sensitivity ($m = \partial \log H / \partial \log \dot{\varepsilon}_L$), where H is the hardness. Figure 2(a) shows the $\log H$–$\log \dot{\varepsilon}_L$ curves obtained for the measurements of NC Cu with different grain sizes. The $\log H$–$\log \dot{\varepsilon}_L$curves exhibit two distinct linear regimes with their slopes at $d = 24.4$ nm, i.e., the m values are 0.086 at $\dot{\varepsilon}_L \leq 2\times10^{-2}$ s^{-1} and 0.035 at $\dot{\varepsilon}_L \geq 2\times10^{-2}$ s^{-1}. Such dependence of m on $\dot{\varepsilon}_L$ is consistent with that found in the indentation test[5] and compression test[13] on NC Cu. With the increase in grain sizes, the $\log H$–$\log \dot{\varepsilon}_L$ curves exhibit one linear regime with their slopes. The average m values over the entire range of $\dot{\varepsilon}_L$ increase from 0.027 to 0.061, which is consistent with the magnitude and general trend of m values reported in Ref. [11] ($m = 0.032$–0.060 for NC Cu). Figure 2(b) presents the variation of m as a function of d for NC Cu including the data resulting from various testing methods.[10,11,20–22,25] Despite some inconsistency in the absolute values obtained using different synthesis techniques or different testing methods, a consistent trend is clear: m values increase slightly with decreasing d from the macro to the submicron scale (from 0.006 to about 0.02), while an obvious "take-off" appears when d decreases to 100 nm or smaller. The m value increases from about 0.02 at $\sim$ 100 nm to about 0.07 at $\sim$ 20 nm.

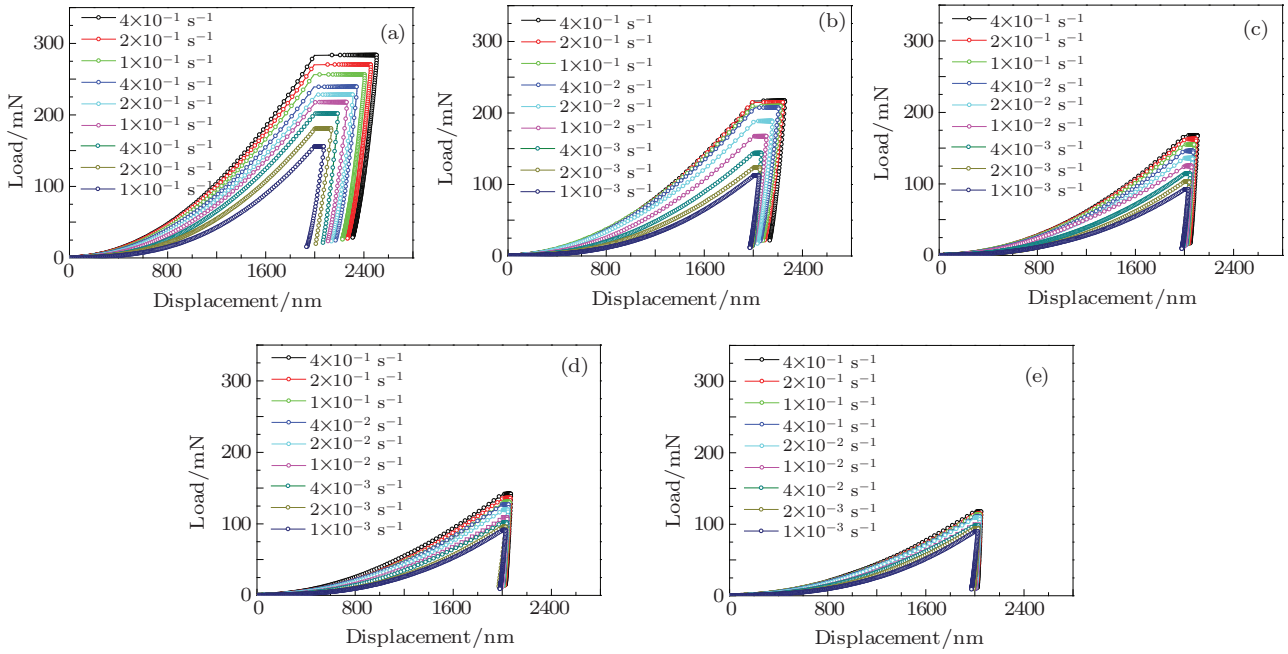


Fig. 1. (color online) Load–displacement (P–h) curves from nanoindentation experiments performed at nine different loading strain rates for NC Cu with (a) $d = 24.4$ nm; (b) $d = 53.7$ nm; (c) $d = 71.2$ nm; (d) $d = 93.3$ nm, and (e) $d = 131.3$ nm.

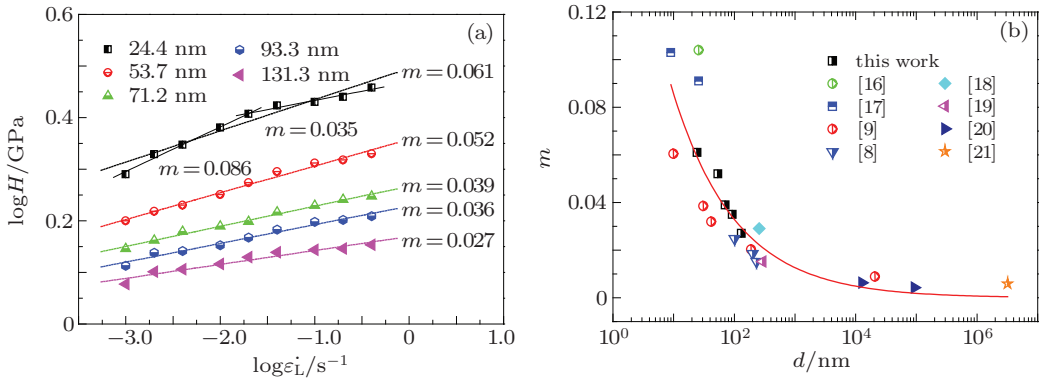


Fig. 2. (color online) (a) Hardness versus loading strain rate ($\log H$–$\log \dot{\varepsilon}_{\rm L}$) curves for measuring the strain rate sensitivities (m) of the NC Cu samples with different grain sizes. (b) Variation of m as a function of d for Cu. Data are from experimental work[10,11,20–25] and this work.

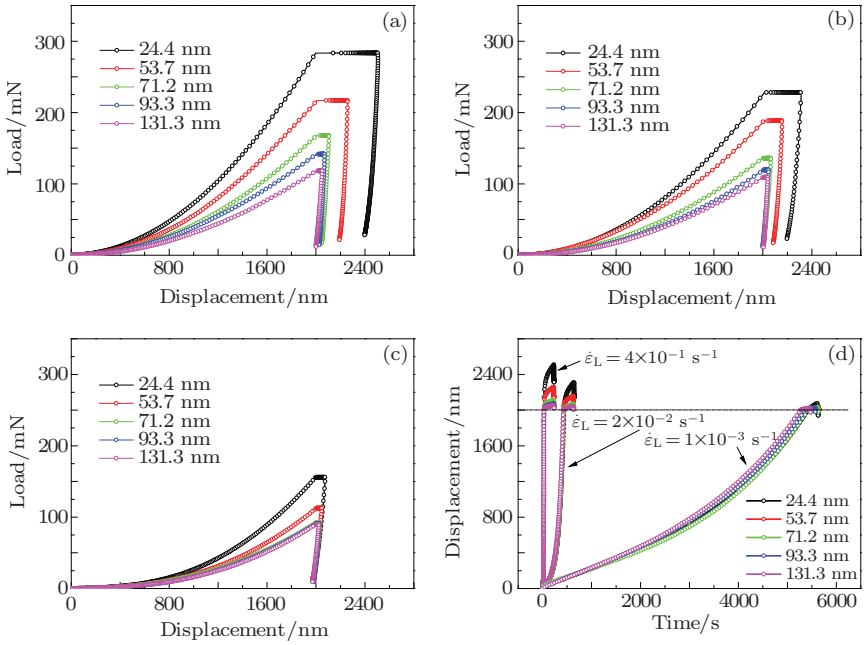


Fig. 3. (color online) Load–displacement (P–h) curves obtained for different grain sizes and strain rates (a) $\dot{\varepsilon}_{\rm L} = 4\times10^{-1}$ s^{-1}; (b) $\dot{\varepsilon}_{\rm L} = 2\times10^{-2}$ s^{-1}; (c) $\dot{\varepsilon}_{\rm L} = 1\times10^{-3}$ s^{-1}. (d) The corresponding displacement–time (h–t) curves.

Figures 3(a)–3(c) show the representative P–h curves obtained for the Cu samples at fixed $\dot{\varepsilon}_L$, and the corresponding displacement-time (h–t) curves are shown in Fig. 3(d). With decreasing grain sizes, a higher indentation load was required in order to impose the same displacement. A significant grain size effect can thus be seen for the NC Cu samples at high $\dot{\varepsilon}_L$. However, the NC Cu samples do not show any strong sensitivity to grain size at low $\dot{\varepsilon}_L$ (see Fig. 3(c)). Figure 4(a) shows the hardness as a function of $d^{-1/2}$. For comparison, the H–P relation extrapolated from the CG Cu[11] is also shown. Most hardness data of the NC Cu are higher than the H–P line. The slopes of hardness versus $d^{-1/2}$, i.e., the k value of H–P relation, is increasing with increasing $\dot{\varepsilon}_L$, as shown in Fig. 4(b) ($k = 4641.08 + 755.62 \log \dot{\varepsilon}_L$).

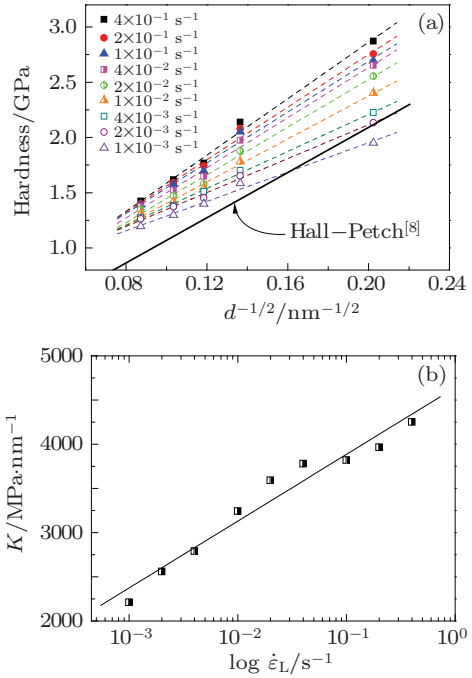


Fig. 4. (color online) (a) Variations of hardness with $d^{-1/2}$ for our Cu samples, the straight lines represent the H–P relation extrapolated from the CG Cu.[11] (b) Variations of the k value of H–P relation with $\dot{\varepsilon}_L$.

3.1.2. Creep process for the NC Cu

In the holding regime, the P–h curves at small grain size and/or high $\dot{\varepsilon}_L$ exhibit significant load plateaus, as shown in Fig. 5. Such variation of holding plateau indicates a decrease in grain size and/or increase in $\dot{\varepsilon}_L$ lead to indenter displacement or a significant creep deformation in the holding regime, which can be also seen in the corresponding h–t curves (see Fig. 3(d). The width of the holding plateau or the indenter displacement reaches the maximum value of $\sim$ 505.9 nm at $d = 24.4$ nm and $\dot{\varepsilon}_L = 4\times10^{-1}$ s^{-1}. Thus, the wide load plateau produced in such a short holding time was not reported in previous nanoindentation creep tests on NC metals.[21,26] To evaluate the creep deformation observed above, the h–t curves after loading were taken from Fig. 3(d) and plotted in Fig. 6(a) as a function of holding time. By fitting the h–t data in the holding regime in Fig. 6(a), the relationship of creep strain ($\varepsilon_H = \triangle h/h$, $\triangle h = (h - 2000)$ nm)[27] with time was determined and plotted in Fig. 6(b) as a function of holding time, together with the experimental data of ε_H. Very good agreement with the experimental data allow us to derive the creep strain rate ($\dot{\varepsilon}_H = (\mathrm{d}h/\mathrm{d}t)/h$)[27] by differentiating the ε_H–t curves in Fig. 6(b), which are plotted in Fig. 6(c) as a function of the holding time. It is seen from Figs. 6(b) and 6(c) that an initial transition regime exists, in which ε_H increases rapidly as the holding time increases and the corresponding $\dot{\varepsilon}_H$ drops rapidly. After a holding time of $\sim$ 100 s, a steady-state creep process occurs, which is characterized by a stable increase in ε_H and a slow decrease in $\dot{\varepsilon}_H$ with increasing holding time. At given holding time, ε_H and $\dot{\varepsilon}_H$ increase with decreasing grain sizes and/or increasing $\dot{\varepsilon}_L$. At a holding time of 200 s, the largest ε_H at $d = 24.4$ nm and $\dot{\varepsilon}_L = 4\times10^{-1}$ s^{-1} is $\sim$ 20%, which is $\sim$ 12 times as high as the largest grain size (131.3 nm) at $\dot{\varepsilon}_L = 4\times10^{-1}$ s^{-1} and $\sim$ 6 times as high as the lowest $\dot{\varepsilon}_L$=1×10^{-3} s^{-1} at $d = 24.4$ nm. At zero holding time, the highest $\dot{\varepsilon}_H$ at $d = 24.4$ nm and $\dot{\varepsilon}_L = 4\times10^{-1}$ s^{-1} is $\sim 3\times10^{-2}$ s^{-1}, which is higher than the largest grain size (131.3 nm) at $\dot{\varepsilon}_L = 4\times10^{-1}$ s^{-1} by $\sim$ 1.7 orders, and higher than the lowest $\dot{\varepsilon}_L$ (1×10^{-3} s^{-1}) at $d = 24.4$ nm by $\sim$ 2.2 orders. In addition, it is noted that $\dot{\varepsilon}_H$ at zero holding time is always smaller than the corresponding $\dot{\varepsilon}_L$.

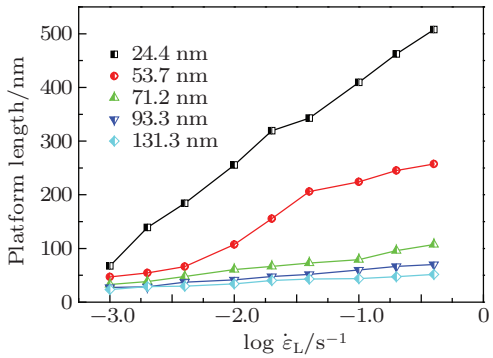


Fig. 5. (color online) Variations of the platform lengths in the holding regime with $\dot{\varepsilon}_L$.

Under constant load, an increase in indenter displacement corresponds to an increase in the contact area of the indenter tip/sample, and thus a decrease in hardness or stress. From the relation of $H = P/(ch^2)$,[27] a simple expression for the stress in the holding regime (σ_H) can be derived, i.e., $\sigma_H = (H/3)(h_0/h)^2$, where H is the hardness, P is the load, h is the contact depth, c is a constant that depends upon the geometry of the indenter (24.56 for the perfect Berkovich geometry) and $h_0 = 2000$ nm is the indenter depth imposed in the loading regime. Using this expression and the experimental h–t data in Fig. 6(a), σ_H–t curves were calculated and plotted in Fig. 6(d). It is seen that σ_H drops with increasing holding time and a larger dropping rate was found at small grain sizes and/or large $\dot{\varepsilon}_L$, indicating a more rapid stress relaxation.

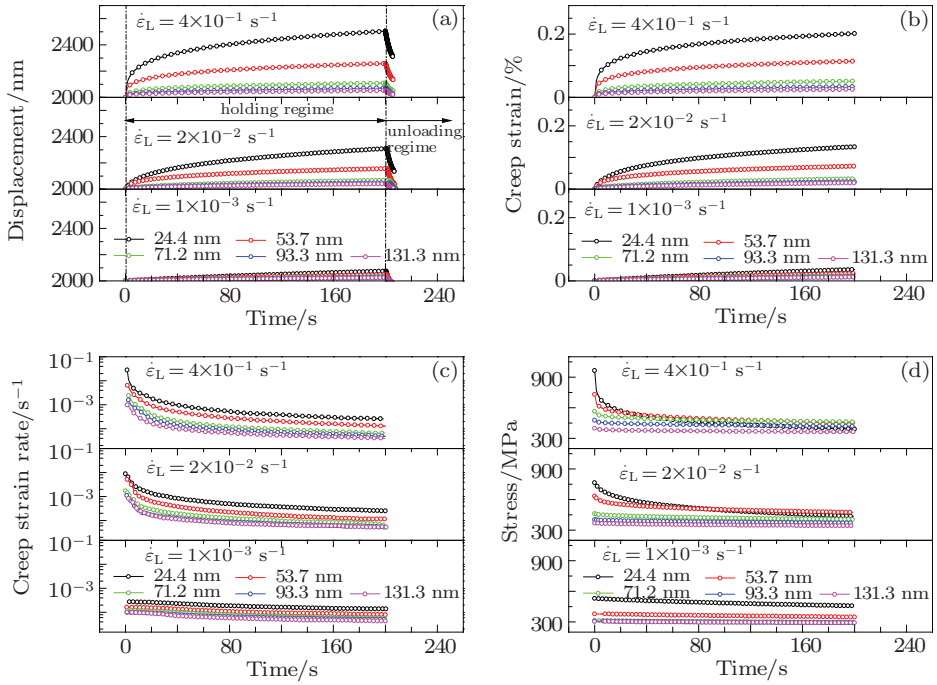


Fig. 6. (color online) (a) Displacement-time (h–t) curves in the holding and unloading regimes; (b) variations of creep strain with holding time in the holding regime; (c) variations of the creep strain rate with holding time in the holding regime; (d) variations of the stress with holding time in the holding regime.

3.2. Microstructures of as-prepared and deformed samples

Figures 7(a)–7(e) show the TEM images and the corresponding statistical distribution results analyzed on about 200 grains of the as-brush-plated NC Cu, which reveal that the average grain sizes are 24.4 nm, 53.7 nm, 71.2 nm, 93.3 nm, and 131.3 nm, respectively. These brushed-plated Cu consist of uniformly equiaxed grains with random crystalline orientations and predominant high-angle GBs. As shown in Fig. 7, more growth twinning could be found in the NC Cu with larger grain size, which is consistent with our recent research[19] on the same NC Cu.

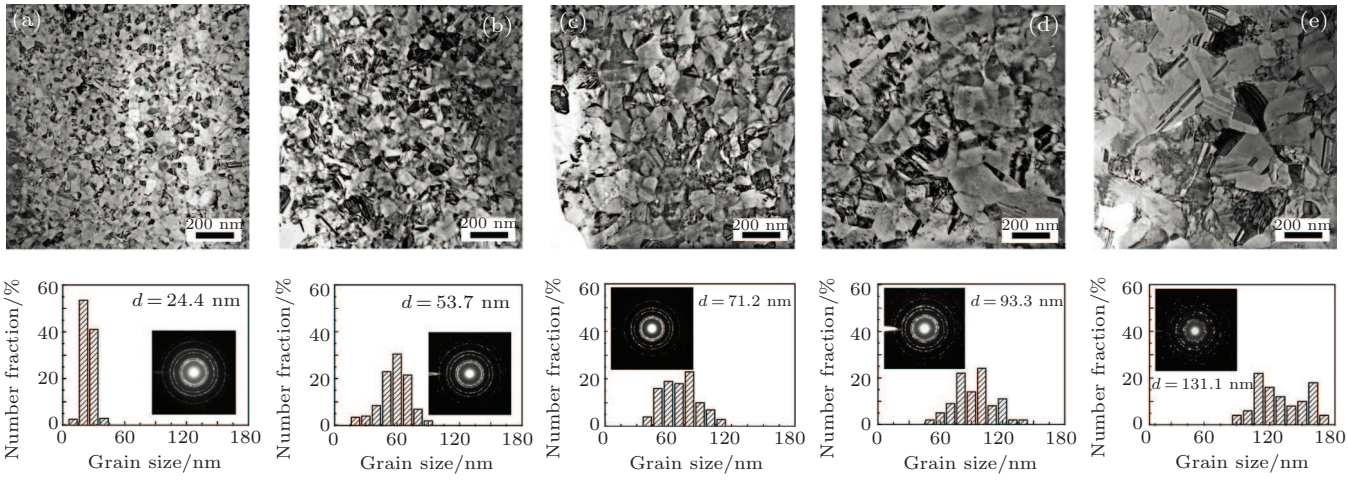


Fig. 7. TEM images and statistical distributions of the grain size for NC Cu with the corresponding selected area diffraction patterns in the as-deposited state prepared using different current densities and concentration of $CuSO_4$ ions in baths (a) 1338.6 mA/cm^2, 300 g/l; (b) 690.3 mA/cm^2, 300 g/l; (c) 251.8 mA/cm^2, 300 g/l; (d) 251.8 mA/cm^2, 200 g/l; (e) 251.8 mA/cm^2, 100 g/l.

The above deformation activities that occurred in loading and holding regimes may result in some local motion of GBs and hence trigger possible grain growth[28] or refinement[29] in the regions near the indenter, which would affect the deformation behavior discussed in the following. Figure 8(a) shows the SEM image of indentation array ($\dot{\varepsilon}_L = 4\times10^{-1}$ s^{-1}) for the NC Cu with $d = 24.4$ nm after ion thinning. The indentation with thin region was shown in Fig. 8(b). Figure 8(c) shows the TEM images of this indentation. Figure 8(d) is the magnified image of the white frame shown in Fig. 8(c) near the indenta-

tion, which confirms that the grain size underneath the indenter has not changed remarkably even after a creep period of 200 s and a higher loading strain rate of 4×10^{-1} s^{-1}. The average grain size of the NC Cu beneath the indenter can be estimated statistically to be about 26 nm, which indicates that no obvious grain growth occurred beneath the indenter. Accordingly, the grain size of the Cu sample was assumed to be constant during the entire creep test. Similar TEM results were also found in the recent indentation tests on the same brush-plated NC Cu samples.[5] The role of a small amount of impurities in stabilizing the grain structure of NC metals has been reported many times. For instance, the nanoindentation creep test result from Zhang *et al.*[28] showed that the grain size of NC Cu with a purity of 99.99% increases significantly during the holding period. Conversely, the grain growth is suppressed when its purity is reduced to 99.6%. Thus, the stable grain structure of our NC Cu may be attributed to its relatively low purity ($\sim$ 99.7%) and predominant high-angle GBs. At low $\dot{\varepsilon}_{\rm L}$, since the GB dislocation sources cannot be activated effectively, the dominant GB sliding in this case would not lead to a substantial increase in the average grain size. Figure 8(e) shows the typical TEM image of NC Cu with d = 131.3 nm after being indented at $\dot{\varepsilon}_{\rm L}$=$4\times10^{-1}$ s^{-1}. The grain size did not show detectable growth near the indenter, indicating that the grain structure remains stable at large grain size. Some twins were found in the grains near the indenter. A high-resolution image of the boxed region together with its Fourier transformation is shown in Fig. 8(f), indicating the twinning relationship.

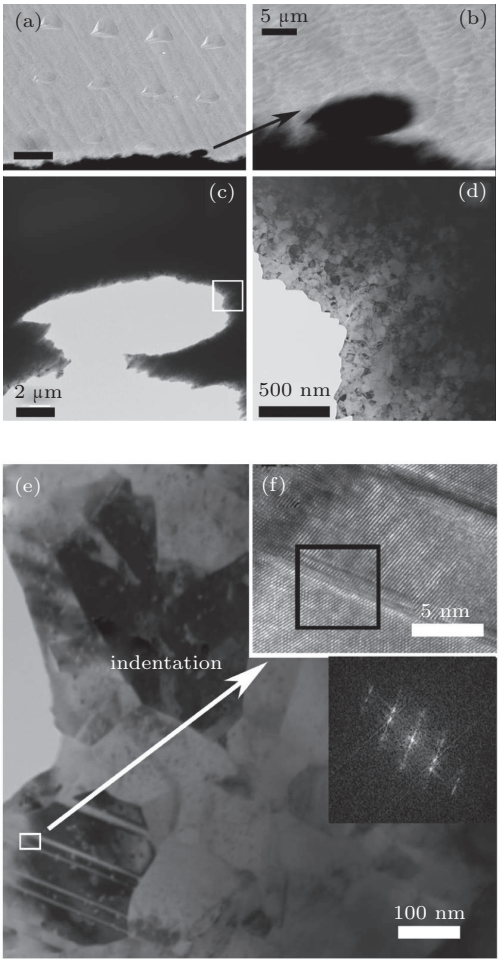


Fig. 8. (a) SEM image of the indentation array ($\dot{\varepsilon}_{\rm L} = 4\times10^{-1}$ s^{-1}) for the NC Cu with d = 24.4 nm after ion thinning; (b) magnified image of the indentation with thin region; (c) the corresponding TEM image; (d) the magnified image of the boxed region in (c); (e) the TEM image obtained for the NC Cu with d = 131.3 nm after being indented at $\dot{\varepsilon}_{\rm L} = 4\times10^{-1}$ s^{-1}; (f) the high-resolution TEM image of the region containing the twins and the corresponding diffraction pattern of the black frame (inset).

4. Discussion

4.1. Creep mechanism for the NC Cu

It has been widely accepted that Coble creep and GB sliding accommodated by thermally activated GB diffusion are two possible mechanisms responsible for the creep behavior of NC metals even at room temperature due to the high volume fractions of GBs and triple junctions.[9,20,21] The creep strain rates produced by these two mechanisms can be, respectively, calculated by the following two equations:[30,31]

$$\dot{\varepsilon}_{\rm Coble} = \frac{148\delta\Omega}{\pi d^3 kT} D_{\rm gb0} \exp\left(-\frac{Q_{\rm gb}}{kT}\right)\sigma, \tag{3}$$

$$\dot{\varepsilon}_{\rm GBS} = 2\times10^5 D_{\rm gb0} \exp\left(-\frac{Q_{\rm gb}}{kT}\right)\left(\frac{Gb}{kT}\right)\left(\frac{b}{d}\right)^3\left(\frac{\sigma}{G}\right)^2, \tag{4}$$

where δ is the GB thickness, Ω is the atomic volume, d is the grain diameter, k is the Boltzmann constant, T is the absolute temperature, $D_{\rm gb0}$ is the frequency factor, $Q_{\rm gb}$ is the activation energy for GB diffusion, σ is the stress, G is the shear modulus, and b is the Burgers vector. In the present calculations, Chokshi *et al.*'s creep result of $Q_{\rm gb}$ = 0.94 eV on NC Cu[32] was used. This $Q_{\rm gb}$ value is close to another result of $Q_{\rm gb}$ = 0.98 eV derived by Conrad[9] based on Cai *et al.*'s creep data on NC Cu.[33] Inserting $Q_{\rm gb}$ = 0.94 eV, T = 298 K, and other material parameters,[34] $b = 2.56\times10^{-10}$ m, $\delta = 4b$, $\Omega = 1.3\times10^{-29}$ m^3, $k = 1.38\times10^{-23}$ Pa$\cdot$m^3/K, $D_{\rm gb0} = 2.35\times10^{-5}$ m$^2\cdot$s^{-1}, $G = 4.21\times10^{10}$ Pa into Eqs. (3) and (4), and using the data of $\sigma_{\rm H}$ in Fig. 6(d), we calculated $\dot{\varepsilon}_{\rm Coble}$ and $\dot{\varepsilon}_{\rm GBS}$. Compared with the derived $\dot{\varepsilon}_{\rm H}$ from experiment, $\dot{\varepsilon}_{\rm Coble}$ and $\dot{\varepsilon}_{\rm GBS}$ are plotted in Figs. 9(a)–9(c) as a function of the grain size for several representative holding times. It can be seen from Figs. 9(a)–9(c) that the calculated $\dot{\varepsilon}_{\rm Coble}$ by Eq. (3) is far smaller than the derived $\dot{\varepsilon}_{\rm H}$. This suggests that the Coble creep should be ruled out as dominant creep mechanism. The calculated $\dot{\varepsilon}_{\rm GBS}$ by Eq. (4) is close to the derived $\dot{\varepsilon}_{\rm H}$ at small grain sizes when the holding time is larger than $\sim$ 100 s, but is far smaller than the derived $\dot{\varepsilon}_{\rm H}$ with the increase in grain sizes and/or decrease in holding time. This indicates that the creep behavior in NC Cu with larger grain size and/or the initial transition regime cannot be explained by the GB sliding mechanism. Therefore, a possibility cause

of this creep behavior is the dislocation activity, as analyzed below.

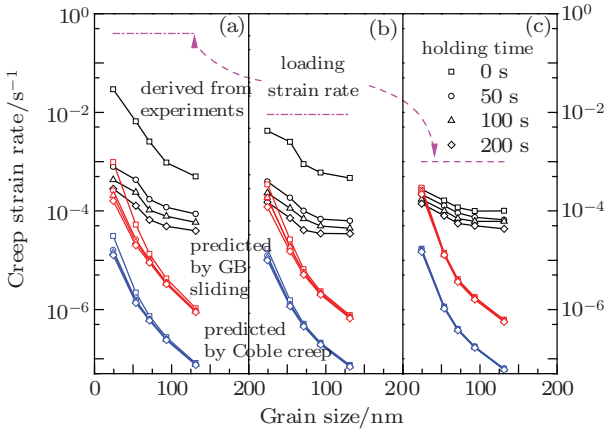


Fig. 9. (color online) Variations of the creep strain rate with the grain sizes derived from experiments and predicted by the models of Coble creep (Eq. (3)) and GB sliding (Eq. (4)) for different holding times and loading strain rate (a) $\dot{\varepsilon}_L = 4.\times10^{-1}$ s^{-1}; (b) $\dot{\varepsilon}_L = 2.\times10^{-2}$ s^{-1}; (c) $\dot{\varepsilon}_L = 1.\times10^{-3}$ s^{-1}.

4.1.1. Creep behavior for the NC Cu with small grain size

For the NC Cu with small grain sizes ($\sim$ 24.4 nm), both dislocation and GB-mediated mechanisms are likely to be activated in the loading regime considering the range of $\dot{\varepsilon}_L$ used in our nanoindentation test and the grain size of this NC Cu ($\sim$ 24.4 nm) that is larger than the critical grain size for the transition from dislocation activity to mechanically activated or stress-driven GB sliding (e.g., $\sim$ 12 nm for Cu[1]). For the dislocation-mediated mechanism, a high shear stress is required for (partial) dislocations to nucleate and emit from GBs.[35] This stress condition cannot be, however, satisfied well at low $\dot{\varepsilon}_L$ because of the stress relaxation role due to the GB-mediated mechanisms, such as the GB sliding accommodated by thermally activated GB diffusion. This GB sliding would preferentially initiate at low $\dot{\varepsilon}_L$ due to its low threshold stress and become the dominant mechanism accommodating applied plastic strain. As $\dot{\varepsilon}_L$ increases, this GB sliding would be suppressed due to the increased difficulty for GB diffusion. A much higher stress is thus needed for the GB sliding to proceed until a much higher strain rate at which the dislocation mechanism is activated.[5] This conclusion is supported by the variation in m with $\dot{\varepsilon}_L$ for the NC Cu with $d = 24.4$ nm, as shown in Fig. 2(a). Such a variation in m with $\dot{\varepsilon}_L$ is attributed to a gradual transition of deformation mechanism from the dominant GB sliding at $\dot{\varepsilon}_L \leq 2\times10^{-2}$ s^{-1} to one governed mainly by the GB emission–absorption mechanism of dislocations at $\dot{\varepsilon}_L \geq 2\times10^{-2}$ s^{-1}. Such a transition of deformation mechanism with strain rate was also predicted by numerical models.[36,37] The emitted dislocations from GBs would propagate across the grains and be eventually absorbed in the opposite GBs. MD simulations[38] have suggested that the dislocation propagation would be hindered by GB pinning points such as GB edges, which must be overcome by thermal activation. Furthermore, the dislocation absorption would involve the rearrangement of the dislocation structure at/near GBs,[39] which also needs the assistance of atomic diffusion. Thus, the dislocation propagation and absorption would also be dependent on $\dot{\varepsilon}_L$. By considering atomic jump or migration between the dislocation core and GB, a theoretical expression for the possibility of a dislocation absorbed by GB (P_{dis}) was derived by Carlton and Ferreira.[40] According to this expression, a low strain rate can result in a large P_{dis} and, in contrast, a high strain rate can promote a small P_{dis}. Therefore, at high loading strain rate, an effective dislocation accumulation or storage would occur during the repeated dislocation nucleation–absorption process due to the enhanced dislocation nucleation and the increased difficulties for the dislocation absorption.

The dislocation structure formed in the loading regime is highly unstable and will break down upon holding in constant load due to a sudden change in deformation mode or a sudden taking off of the continuous supporting of applied strain rate. Since the stress level and state persist in the initial holding regime, the stored dislocations will still propagate forward and produce plastic strain, i.e., the creep strain, when they are absorbed in the opposite GBs. Furthermore, since the stress condition for dislocation nucleation can be still satisfied well in the initial holding regime for $\dot{\varepsilon}_L \geq 2\times10^{-2}$ s^{-1}, new dislocations are able to continue to nucleate from GBs and produce the creep strain in the same way in which dislocations are stored. The shear strains produced by the above dislocation absorption processes can be estimated to be $\gamma = (b/d)/2$ and $\gamma = b/d$ for the stored and newly nucleated dislocations, where b is the burgers vector, and d is the grain size. This indicates that the high-speed creep process observed above is mediated mainly by the rapid absorptions of the stored and newly nucleated dislocations, the larger ε_H and $\dot{\varepsilon}_H$ at small grain sizes arise from the larger strain produced by the absorption of dislocations due to a larger b/d value. For the dislocation-mediated mechanism, a high shear stress is required for dislocations to nucleate and emit from GBs.[35] With the increase in holding time ($>$ 100 s), this stress condition cannot be satisfied because of the stress relaxation role, which is caused by the GB-mediated mechanisms, such as the GB sliding accommodated by thermally activated GB diffusion (see Fig. 6(d)). As the number of emitted dislocations and the stress level drops, the high-speed creep process mediated by the rapid dislocation absorption will slow down and is gradually replaced by the slow creep process mediated mainly by the thermally activated GB sliding. At low $\dot{\varepsilon}_L$ (e.g., $\dot{\varepsilon}_L \leq 2\times10^{-2}$s^{-1}), fewer or no dislocations can be stored in the loading regime, and the thermally activated GB sliding becomes the dominant mecha-

nism responsible for the very small ε_H and $\dot{\varepsilon}_H$ observed in the entire holding regime.

According to the above expression, at small grain sizes and high $\dot{\varepsilon}_L$, an effective dislocation accumulation or storage would occur during the repeated nucleation–absorption process of dislocations due to the enhanced dislocation nucleation and the increased difficulties for the dislocation absorption. A high internal (back) stress would thus develop inside the grain due to the inhomogeneous distribution of the stored dislocations inside the grain[39] and/or the possible formation of the dislocation pile-ups against the opposite GBs.[1] Obviously, such dislocation structure cannot form at large grain size and low $\dot{\varepsilon}_L$ (e.g., $\dot{\varepsilon}_L \leq 2\times10^{-2}$ s^{-1}), and fewer dislocations emitting from GBs would be trapped at/near GBs to form thin GB-affected zone.

4.1.2. Creep behavior for the NC Cu with large grain size

As the grain size increases, this GB sliding and/or Coble creep would be suppressed due to the reduced difficulty for dislocation activity, as shown in Fig. 9. A mechanistic model for NC metals has been developed by Asaro and Suresh[35] in terms of the emission of dislocations at a stress concentration at GBs. They observed that the emission of dislocations from GBs is easier for the metal with larger grain sizes. Meanwhile, the energy barrier for nucleating dislocation is lower in the materials with lower stacking fault energy.[41] As we know, Cu is a low stacking fault energy material. Hence, the dislocation activity in NC Cu with larger grain sizes is more active. This conclusion coincides with our measured values of m for the NC Cu samples (see Fig. 2(a)), which decreases monotonically with the increasing of grain sizes. This suggests that dislocation-mediated mechanism should be considered as dominant creep mechanism in coarser grained materials. For the NC Cu with larger grain sizes, more dislocations can be emitted within one grain in the loading and holding regimes. Therefore, the effect of small number of dislocations piling up at/near GBs should be considered, which may hinder further movement of dislocations. In addition, the growth twins in the NC Cu with larger grain size shown in Fig 7, could also act as a barrier for the dislocations sliding. As reported recently, in the nanocrystalline grain size regime, there is a larger deformation twinning propensity,[42] when the grain size increases to a critical size (to Cu, $\sim$ 80 nm). Partial dislocation emissions from grain boundaries are possible even in grains of NC Cu as large as $\sim$ 200 nm,[8,43] which leads to the formation of deformation twins. The above results are consistent with our TEM observation, shown in Figs. 7(e) and 7(f), there are more twins in the grains near the indenter of the NC Cu with larger grain size. In this size range (from $\sim$ 80 nm to $\sim$ 200 nm), the full dislocation motion is effectively blocked by the twins generated by partial dislocation emission from the grain boundaries. As a result, the dislocation storage capacity is maintained in the loading regime of NC Cu. However, because the twins act as effective sites for blocking slipping dislocations in the holding and unloading regime, the storing dislocations during loading period could not propagate forward and/or absorb in the opposite GBs. Consequently, in the NC Cu with larger grain sizes, the dislocation structure formed in the loading and holding regimes is more stable. Under such conditions, no significant plastic strain can be observed.

5. Conclusion

Nanocrystalline Cu with average grain sizes ranging from $\sim$ 24.4 to 131.3 nm were successfully prepared by the electric brush-plating technique. During holding with a constant load in the nanoindentation test, a creep process mediated by rapid dislocation absorption was found in brush-plated NC Cu. The dislocation activities in NC Cu have strong grain size and loading strain rate dependence. The creep process observed at small grain sizes and high loading strain rate in the initial transition regime is mediated mainly by the rapid absorptions of these stored dislocations. This dislocation-mediated creep process is replaced gradually by the slow creep process mediated mainly by the thermally activated GB sliding. With the increase in grain size and/or decreasing of loading strain rate, the above dislocation absorption process becomes not obvious and the small creep strain and creep strain rate are mainly due to the dislocations interaction and deformation twinning for large grain size and GB-mediated mechanisms for low loading strain rate.

Acknowledgements

The authors thank Dr. Hu Jiang for experimental assistance and Han Shuang for helpful discussion.

References

[1] Schiøtz J and Jacobsen K W 2003 *Science* **301** 1357
[2] Kumar K, Van Swygenhoven H and Suresh S 2003 *Acta Mater.* **51** 5743
[3] Wolf D, Yamakov V, Phillpot S, Mukherjee A and Gleiter H 2005 *Acta Mater.* **53** 1
[4] Shao Y F, Yang X, Zhao X and Wang S Q 2012 *Chin. Phys. B* **21** 083101
[5] Mu J W, Jiang Z H, Zheng W T, Tian H W, Lian J S and Jiang Q 2012 *J. Appl. Phys.* **111** 063506
[6] Gu C D, Lian J S, Jiang Q and Zheng W T 2007 *J. Phys. D* **40** 7440
[7] Li P Y, Zhang X Y, Ni H T, Cao Z H and Meng X K 2012 *Chin. Phys. Lett.* **29** 026201
[8] Yue Y H, Wang L H, Zhang Z and Han X D 2012 *Chin. Phys. Lett.* **29** 066201
[9] Conrad H 2003 *Mater. Sci. Eng. A* **341** 216
[10] Wei Q, Cheng S, Ramesh K and Ma E 2004 *Mater. Sci. Eng. A* **381** 71
[11] Chen J, Lu L and Lu K 2006 *Scripta Mater.* **54** 1913
[12] Zhang J M and Xu K W 2004 *Acta Phys. Sin.* **53** 2439 (in Chinese)
[13] Wang G Y, Lian J S, Jiang Z H, Qin L Y and Jiang Q 2009 *J. Appl. Phys.* **106** 086103
[14] Khan A S, Farrokh B and Takacs L 2008 *J. Mater. Sci.* **43** 3305
[15] Zhang X, Fujita T, Pan D, Yu J, Sakurai T and Chen M 2010 *Mater. Sci. Eng. A* **527** 2297

[16] van Swygenhoven H 2002 *Science* **296** 66

[17] Imran M, Hussain F, Rashid M and Ahmad S A 2012 *Chin. Phys. B* **21** 126802

[18] Shao Y F, Zhao X, Li J H and Wang S Q 2013 *Comput. Mater. Sci.* **67** 346

[19] Mu J W, Zhao L, Sun S C, Jiang Z H and Lian J S 2012 *Integr. Ferroelectr.* **137** 52

[20] Jiang Z H, Liu X L, Li G Y, Jiang Q and Lian J S 2006 *Appl. Phys. Lett.* **88** 143113

[21] Huang P, Wang F, Xu M, Xu K and Lu T 2010 *Acta Mater.* **58** 5196

[22] Elmustafa A A, Tambwe M F and Stone D S 2002 *Surface Engineering 2002-Synthesis, Characterization and Applications* December 2, 2002 Boston, USA, p.Y8.14.1

[23] Gray G, Lowe T, Cady C, Valiev R and Aleksandrov I 1997 *Nanostruct. Mater.* **9** 477

[24] Carreker R and Hibbard W 1953 *Acta Metall.* **1** 654

[25] Bochniak W 1995 *Acta Metall. et. Mater.* **43** 225

[26] Cao Z, Lu H, Meng X and Ngan A 2009 *J. Appl. Phys.* **105** 083521

[27] Lucas B and Oliver W 1999 *Metall. Mater. Trans. A* **30** 601

[28] Zhang K, Weertman J and Eastman J 2005 *Appl. Phys. Lett.* **87** 061921

[29] Zou Y T, Lei L, Wang Z, Wang J H, Zhang W and He D 2009 *Chin. Phys. B* **18** 815

[30] Coble R 1963 *J. Appl. Phys.* **34** 1679

[31] Lüthy H, White R A and Sherby O D 1979 *Mater. Sci. Eng.* **39** 211

[32] Chokshi A, Rosen A, Karch J and Gleiter H 1989 *Scripta Metall.* **23** 1679

[33] Cai B, Kong Q, Lu L and Lu K 1999 *Scripta Mater.* **41** 755

[34] Valiev R, Kozlov E, Ivanov Y F, Lian J, Nazarov A and Baudelet B 1994 *Acta Metall. et. Mater.* **42** 2467

[35] Asaro R J and Suresh S 2005 *Acta Mater.* **53** 3369

[36] Wei Y J and Gao H J 2008 *Mater. Sci. Eng. A* **478** 16

[37] Wei Y J, Bower A F and Gao H J 2008 *Acta Mater.* **56** 1741

[38] Van Swygenhoven H, Derlet P and Frøseth A 2006 *Acta Mater.* **54** 1975

[39] Wang Y, Hamza A and Ma E 2006 *Acta Mater.* **54** 2715

[40] Carlton C and Ferreira P 2007 *Acta Mater.* **55** 3749

[41] Shao Y F, Yang X, Zhao X and Wang S Q 2012 *Chin. Phys. B* **21** 093104

[42] Zhang J Y, Liu G, Wang R H, Li J, Sun J and Ma E 2010 *Phys. Rev. B* **81** 172104

[43] Wang Z, Wang Y, Liao X, Zhao Y, Lavernia E, Zhu Y, Horita Z and Langdon T 2009 *Scripta Mater.* **60** 52